Pergamon

Cement and Concrete Research 32 (2002) 279–287

CEMENT AND CONCRETE RESEARCH

How to study drying shrinkage microcracking in cement-based materials using optical and scanning electron microscopy?

J. Bisschop*, J.G.M. van Mier

Faculty of Civil Engineering and Geosciences, Delft University of Technology, Microlab, P.O. Box 5048, 2600 GA Delft, The Netherlands

Received 9 January 2001; accepted 20 August 2001

Abstract

Three different 'destructive' microscopy methods were tested on their ability to show drying shrinkage microcracks on a specimen cross-section. The first two were methods in which the microcracks were impregnated with a fluorescent epoxy and examined with fluorescence microscopy. In one method, the impregnation was applied before making the cross-section and in the other after making the cross-section. In the third method, the sample was kept wet constantly and examined in an environmental scanning electron microscope (ESEM). It was concluded that the method in which the dried specimen was impregnated before making the cross-section was the most reliable method to record drying shrinkage microcracks. With this method, it was possible to impregnate the complete drying shrinkage microcrack pattern in the studied cement-based materials from the surface, and there was no risk of recording microcracks introduced by sample preparation.

Keywords: Drying; Shrinkage; Microcracking; Sample preparation; Crack detection

1. Introduction

In cement-based materials, drying shrinkage of the hardened cement paste matrix leads to (eigen)stresses and can lead to cracking if the shrinkage is restrained. There are two types of internal restraints that may cause shrinkage microcracking. Firstly, when moisture is lost from the specimen to the surroundings, a moisture gradient develops across the specimen, causing differential shrinkage. This will lead to so-called self-restraining of a specimen. In hardened cement paste, this phenomenon is accompanied by tensile stresses parallel to the drying surface causing microcracks perpendicular to this surface [1,2]. Secondly, the aggregates, with a higher stiffness than the cement paste matrix, restrain matrix shrinkage. This restraining effect causes radial and tangential stresses around an aggregate particle and results (when large enough) in radial and bond microcracking [2,3]. In the case of drying shrinkage in concrete, the stresses due to both types of restraints are superimposed. In this paper, the term microcrack is used for cracks with width smaller than 50 μm; larger crack widths were not observed in the studied materials.

Different methods have been reported to study microcracking in cement-based materials using optical and scanning electron microscopy (SEM) [4,5]. In a number of studies, it has become clear that due to the moisture sensitivity of cement-based materials, new drying shrinkage microcracks are very easily introduced on the microscope sample surface by drying during sample preparation or examination in SEM [5–9]. When it is not clear which microcracks are the cracks of interest (here called *primary* microcracks), and which cracks are introduced by sample preparation (called *secondary* microcracks), erroneous interpretations can be easily made (Fig. 2). To avoid drying, and thus the introduction of secondary shrinkage microcracks, a number of methods have been developed to apply optical and electron microscopy to study microcracks without drying of the microscope sample [5,6,9,10]. Problems may occur when these methods are used to study primary shrinkage microcracks. When there is interest in the magnitude and the penetration depth of this type of microcracking, a cross-section has to be made through the dried specimen. Normally, a cross-section is made by cutting using cooling

* Corresponding author. Tel.: +31-15278-2301; fax: +31-15278-6383.
E-mail address: j.bisschop@citg.tudelft.nl (J. Bisschop).

0008-8846/02/$ – see front matter
PII: S0008-8846(01)00671-8

water, which results in rewetting of the material. Rewetting causes swelling of the dried cement paste. Consequently, complete or partial closure of microcracks may occur, which then might become difficult to detect [4,9].

In this paper, three 'destructive' microscopy methods have been tested for their ability to show primary drying shrinkage microcracks on a cross-section of a dried specimen. It has been investigated for each method to what extent secondary microcracks are introduced by sample preparation or during examination in environmental SEM (ESEM). The methods are:

1. Impregnation of specimen with fluorescent epoxy *before* making the cross-section [in combination with fluorescence light microscopy (FLM)].
2. Impregnation of sample surface with fluorescent epoxy *after* making the cross-section (in combination with FLM).
3. No impregnation and no drying during sample preparation (in combination with ESEM).

2. Materials and method

2.1. Material and curing conditions

In this study, $40 \times 40 \times 160$ mm prisms of mortar with a water–cement ratio of 0.5 and a cement–sand ratio of 0.5 were investigated. The grading of the sand and the composition of the cement are given in Ref. [8]. After demoulding, the prisms were cured for 6 days in tap water saturated with calcium hydroxide. Subsequently, the prisms were wet-cured or dried to introduce primary drying shrinkage microcracks according to the following conditions:

- Prism A was wet-cured for 14 days in the aforementioned water;
- Prism B was dried in climate box at 12% (±2%) relative humidity (RH) and 30 °C for 14 days;
- Prism C was dried in climate box at 12% (±2%) RH and 30 °C for 10 days and subsequently dried at 105 °C in a furnace for another 4 days.

The moisture loss curves for Prisms B and C are given in Fig. 1. The moisture absorption during the initial 6 days of wet-curing was on average 6.3 g. It was determined (by weight loss measurements) that at the end of the drying experiment Prism B had lost about 32% and Prism C about 64% of their initial water content of about 88 g.

2.2. Sample preparation and microscopes

Three different microscopy methods were tested on their ability to show primary shrinkage microcracks on a cross-section of the dried mortar prisms. The cross-section, which became the microscope sample surface, was made in the center of the prism perpendicular to the longitudinal axis of the prism (see Fig. 2).

To make microcracks clearly visible on a cross-section for optical microscopy, microscope samples were impregnated with a fluorescent epoxy (Compox Harpiks BY 159) in this study. All microcracks and pores that were filled with the fluorescent epoxy illuminate when viewed in the ultraviolet light mode of the optical microscope. So-called fluorescent thin sections are impregnated samples of concrete ground to a thickness of 30 μm. At this thickness, cement-based materials become translucent and can be examined with transmitted light microscopy. Thin sections are made when microcracks with a width of less than 10 μm need to be observed, which is possible at 100× magnification in transmitted light. Making a fluorescent thin section is a laborious procedure existing of many steps. In this section, only some relevant steps of the thin-section preparation will be mentioned (for more details, see Ref. [8]).

For SEM, samples need not be impregnated to improve visibility of microcracks, because open microcracks show large contrast with the surrounding paste in electron micro-

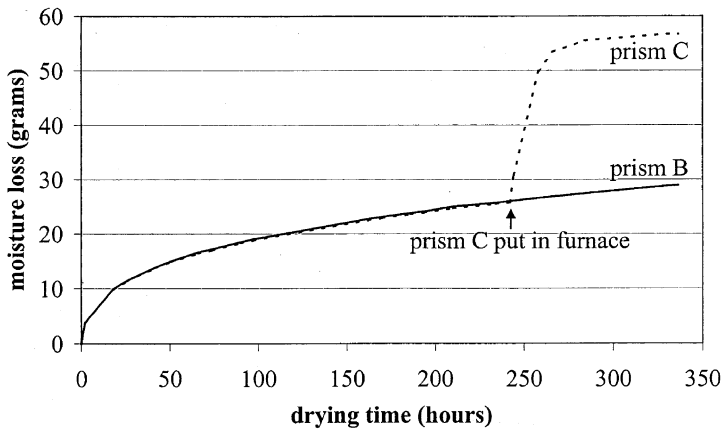

Fig. 1. Moisture loss curves for Prisms B and C during drying at 12% RH and 30 °C. At a drying time of 244 h, Prism C is put in a furnace at 105 °C.

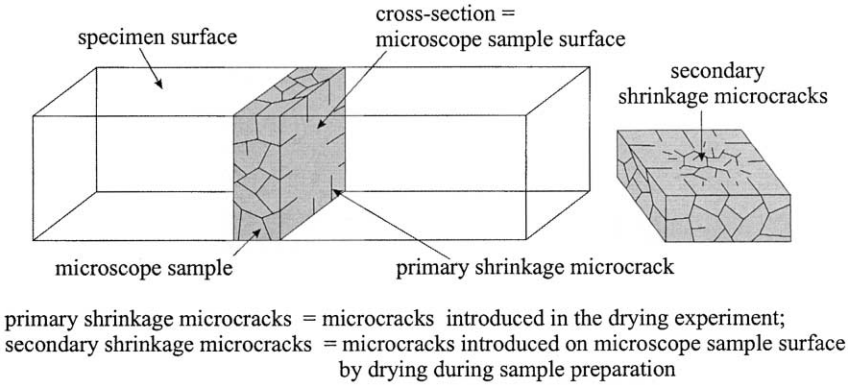

Fig. 2. Nomenclature of microcracks in dried (cement paste) specimen (prism of 40 × 40 × 160 mm) and microscope sample.

scopy (see Figs. 6 and 7). To make microcracks visible, only the rough cut surface had to be ground.

2.2.1. Method 1: impregnation before making the cross-section (FLM)

The simplest and safest way to study primary shrinkage microcracks would be to impregnate the dried prism before making the cross-section. In this way, secondary microcracks caused by cutting, grinding or drying can always be distinguished from the primary shrinkage microcracks. The reason is that secondary microcracks are not filled with fluorescent epoxy and, as such, do not illuminate in UV light. This method only allows impregnating microcracks connected to the surface. Isolated microcracks inside the material cannot be impregnated from the prism surface.

Fluorescent thin sections were made of Prisms B and C after the prisms had been impregnated with the fluorescent epoxy. Impregnation took place in vacuum of approximately 10 mbar for 8 min, which resulted in some additional drying. For Prism B, it was determined that this additional drying was accompanied with 0.1 g moisture loss. Because Prisms B and C were already dried at low RH, the additional drying during vacuum impregnation did probably have a negligible effect on microcracking. In the case of specimens dried at much higher RH, there might be an effect of vacuum impregnation on microcracking, and this needs to be studied further.

After impregnation, a sample as indicated in Fig. 2 was cut out of the prism, which was then further used in the thin-section preparation. The thin sections were examined with a Leica transmitted light microscope in an ultraviolet light mode.

Of thin sections B and C, a single crack map of 10 × 40 mm was made according to a method described in more detail in Ref. [8] (see Fig. 4). In these crack maps, shrinkage microcracks in paste were manually mapped (simplified as straight lines) on a reference image by examination of the thin section at 100 × magnification. The cracks in the crack maps shown in this paper have been dilated for clarity. Shrinkage bond cracks were not plotted. The shrinkage of the paste around aggregates causes radial compressive stresses [3], which may avoid bond cracks to open and therefore they may not be visible. In general, bond cracks open when they are partly caused by self-restraining tensile stresses [2]. Mapping only visible bond cracks will lead to an incomplete picture of the state of bond cracking.

2.2.2. Method 2: impregnation after making the cross-section (FLM)

In Method 2, the prisms are impregnated after making the cross-section. A drawback of this method is that secondary microcracks introduced by sample preparation are also impregnated. If secondary microcracks cannot be separated from the primary shrinkage microcracks, this method cannot be used. To test whether this is the case, fluorescent thin sections were made of Prisms A–C (thin sections AA, BB and CC, respectively), in which the cross-section surface was impregnated after cutting.

Because it was known that rewetting the microscope sample by the cooling water during cutting leads to (partial) closure of primary shrinkage microcracks due to the swelling of the cement paste [4,9], it was decided to cut the prisms without using cooling water. Before impregnation, there is chance of introducing secondary microcracks at a number of steps. Firstly, the cutting itself may lead to the introduction of secondary mechanical microcracks. The microscope sample edges were especially sensitive to the introduction of this type of microcracking as was observed (see Fig. 5a–c). To reduce this type of microcracking, the prism was embedded before cutting [8]. Moreover, the cutting (without cooling water) leads to heat development. This may cause drying and thus the introduction of secondary shrinkage microcracks. Also, the predrying before impregnation and the impregnation itself (in vacuum) may cause secondary shrinkage microcrack formation. In this method, the predrying before impregnation comprised a ½ h drying at 12% RH and 30 °C in a climate box.

To produce a perfectly flat sample surface, the microscope sample is ground after impregnation in the thin-section preparation procedure. Due to grinding (the grinding

depth is the same for all samples), part of the impregnated top layer of the microscope sample is removed. In thin section AA, it can be seen that only the more porous zones (microcracks, air-voids, paste adjacent to microcracks and paste in the interface zone) are impregnated, while in thin section CC, the complete cement paste is impregnated (see Fig. 3). This means that in Prism C the impregnation depth of the epoxy was larger than in Prism A. This resulted in a higher contrast of microcracks in thin section AA in comparison to microcracks in thin section CC. Thin section BB showed a completely impregnated rim (like CC) and a partly impregnated core (like AA).

A crack map was made of the thin sections according to the method described in Section 2.2.1. The secondary microcracks near the sample edges caused by cutting could be clearly separated from the shrinkage microcracks under the microscope. They were simplified by a number of straight line segments including bond cracks (see Fig. 5a–c). The available equipment allows the production of thin sections with an area of 30×40 mm only. Therefore, 10×40 mm of the casting surface side of the sample was removed by cutting (bottom parts of Fig. 5a–c).

2.2.3. Method 3: no impregnation and no drying during sample preparation (ESEM)

Because Method 2 leads to an unwanted introduction of secondary shrinkage microcracks, it was tried to develop a method to observe primary shrinkage microcracks on a cross-section without drying during sample preparation using ESEM [9]. An ESEM is different from conventional SEM by the fact that samples do not have to be coated and evacuated before examination. Moreover, drying of a sample in ESEM can be controlled or even completely avoided [4,9,11]. With this method, the sample is kept wet during sample preparation (cooling water is used during cutting and grinding) until examination in ESEM. As a consequence, primary drying shrinkage microcracks are partially or completely closed because of swelling of the dried cement paste. Therefore, primary shrinkage microcracks may be hard to observe or even may be completely invisible. The extent of crack closure depends on the irreversible shrinkage of the cement paste and on local rotations near the crack face. Although ESEM has a higher resolution than optical microscopy (used in Methods 1 and 2), the scale of observation with both microscopes was taken the same.

ESEM samples were produced of Prisms A and C to investigate whether (partially) closed primary shrinkage microcracks could be seen in ESEM and to see how secondary shrinkage microcracks were introduced by drying in the ESEM chamber. Before cutting, the prisms were thoroughly embedded to minimize introduction of secondary cutting microcracks near the sample edge. The ESEM samples were ground using sandpaper with water and were examined immediately after grinding.

The ESEM samples of Prisms A and C were examined in a Phillips XL30 ESEM-W using a Gaseous Secondary Electron (GSE) detector. The samples were first studied in ESEM using a special device to control the RH above the sample surface [9]. Initially, the RH in ESEM chamber was held between 70% and 100%, at which there was no or slow drying. Subsequently, samples were subjected to severe drying in ESEM chamber for ½ h (and longer) at room temperature (21 °C) and a water vapor pressure of 3.0 Torr, corresponding to a RH of about 15%. In summary, with this method, the material was dried (in a drying experiment), rewetted (during sample preparation and in ESEM) and finally dried (in ESEM to introduce secondary shrinkage microcracks).

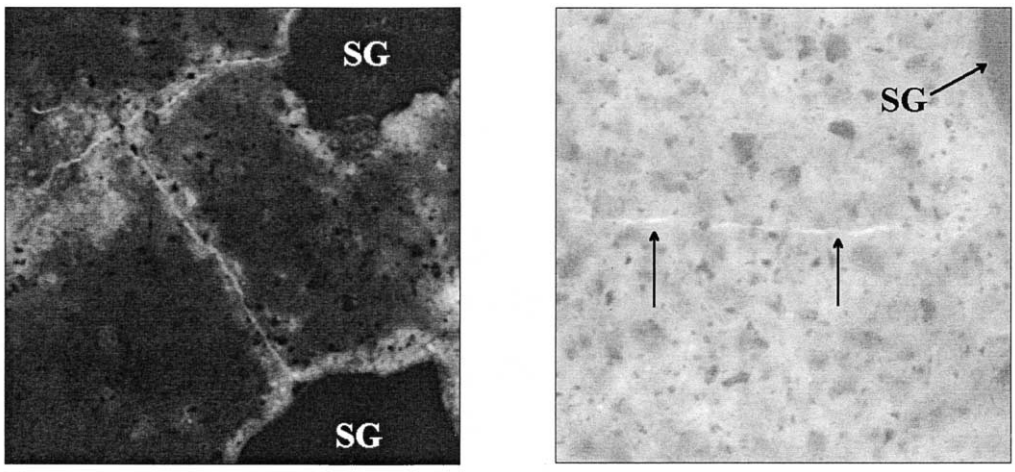

Fig. 3. (a and b) FLM micrographs showing drying shrinkage microcracks in fluorescent thin sections AA and CC, respectively. Note that the cement paste of thin section AA is not completely impregnated, while this is the case in thin section CC. Frame width is 0.3 mm in both images. SG = sand grain.

3. Results

3.1. Observations with Method 1

Fig. 4a and b are FLM micrographs showing the impregnated parts of Prisms B and C prepared according to Method 1. These micrographs show that, due to more extreme drying, Prism C was more impregnated from the surface than Prism B. The microcracks seen in the impregnated part of thin sections B and C at 100 × magnification are primary shrinkage microcracks, and the crack maps showing the distribution of these microcracks are given in Fig. 4c and d. The maximum crack depth measured from these crack maps is 1.5 mm in Prism B and 3.2 mm in Prism C. The total paste crack length is 7.7 mm in Prism B and 24.1 mm in Prism C. The maximum crack width measured in sample C (on surface parallel section) was 30 μm. The impregnated primary shrinkage microcracks have orientations roughly perpendicular to the prism surface.

3.2. Observations with Method 2

The crack maps of the fluorescent thin sections prepared according to Method 2 are given in Fig. 5a–c. The relatively long microcracks near the edge of the thin sections, with an orientation roughly parallel to the prism surface, are secondary cutting microcracks as described in Section 2.2.2. As shown in other materials, damage caused by cutting (i.e. by making the cross-section) is mainly confined to parts near the specimen surfaces [12]. The cutting microcracks had widths of up to 50 μm. This type of microcracking is much more common in thin sections BB and CC than in thin section AA. This is probably due to the following reasons: (1) The dried samples might have had less strength near the edges, because the hydration time was shorter there, and (2) the presence of primary drying shrinkage stresses and microcracks near the prism surface also decreased the strength of the parts near the prism surface. The differences in the degree (and orientation?) of cracking caused by cutting on the three sides is probably related to the cutting direction. More cracks are generally introduced at that side where the cutting is finished.

The relatively short dispersed microcracks without a preferred orientation are shrinkage microcracks, either primary or secondary (Fig. 5a–c). Fig. 3 shows two FLM micrographs of these shrinkage microcracks in thin sections AA and CC. These microcracks were always perpendicular to sand grains, which indicates that they were caused by shrinkage restraint by these sand grains. The shrinkage microcracks have widths of up to 5 μm in thin section AA. In thin section CC, the overall crack width seemed less, but the width of small microcracks (< 5 μm) is difficult to measure in thin sections. The primary shrinkage microcracks that were shown by Method 1 were also impregnated in Method 2. However, they are hard to distinguish in the crack maps because of the overprinting microcrack pattern caused by cutting.

There is a clear difference between the shrinkage microcrack number and distributions in thin sections AA, BB and CC (see Fig. 5a–c): Thin section AA shows most and thin section CC the least microcracks in both samples without preferred distribution. Thin section BB shows a relatively high concentration of microcracks in the center of the thin section and a rim of about 7 mm with much less microcracks.

3.3. Observations with Method 3

When the centers of the ESEM sample of the wet-cured prism (A) and the completely dried prism (C) were examined at a RH of 90–100% in ESEM, no microcracks were seen at all. Even at 70% RH, when drying was slow, no microcracks were found at the start of the examination (Fig. 6a). This indicates that no microcracks were introduced by cutting in the center of the sample. When, subsequently, the RH in the ESEM was lowered to 13%, secondary shrinkage microcracks appeared within a few minutes (Fig. 6b). The typical secondary shrinkage micro-

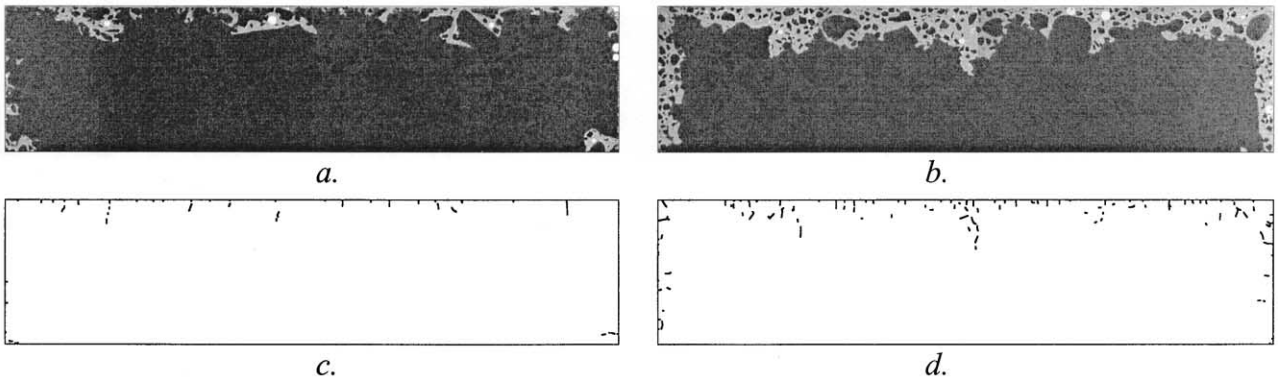

Fig. 4. (a and b) FLM micrographs of 10 × 40 mm of thin sections B and C prepared according to Method 1. (c and d) Microcrack maps (obtained by manual crack mapping at 100 × magnification) showing primary shrinkage microcracks in thin sections B and C, respectively.

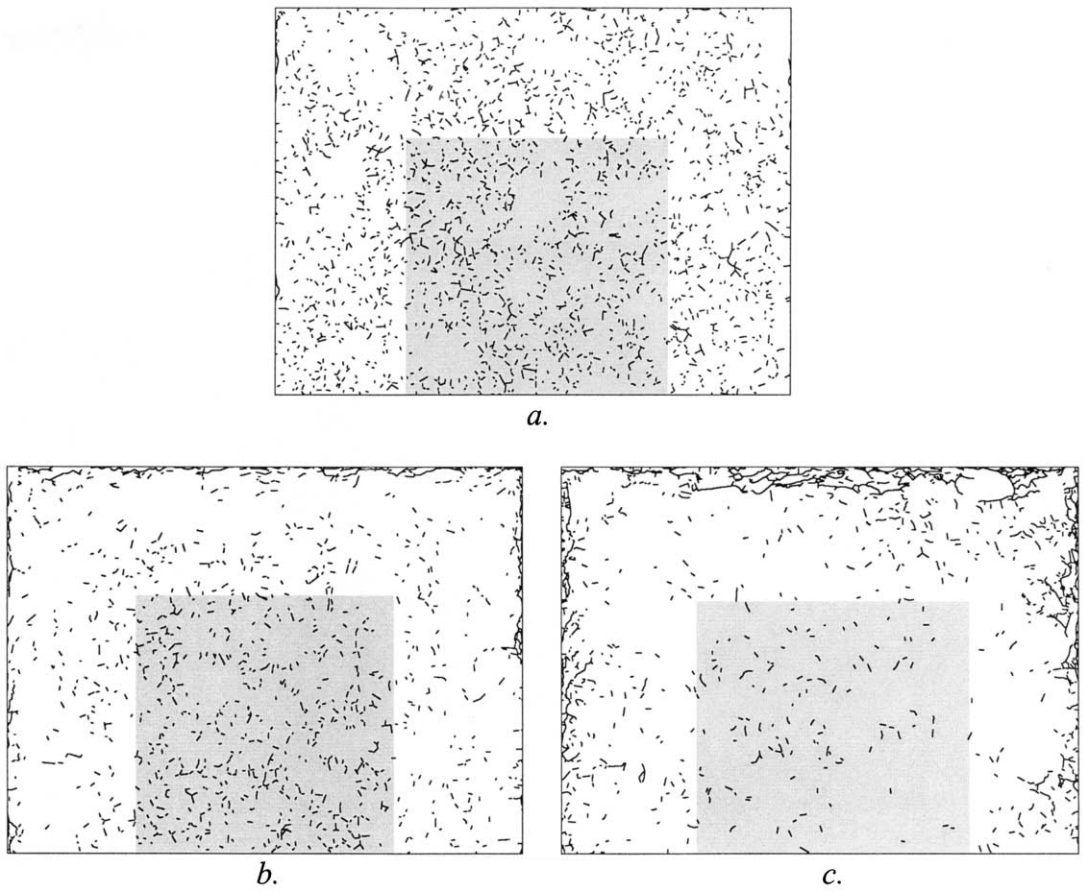

Fig. 5. (a–c) Microcrack maps of 30 × 40 mm showing shrinkage and sawing microcracking in fluorescent thin sections AA, BB and CC, respectively. Number of shrinkage microcracks in middle part of cross-section (grey square with area of 20 × 20 mm) is AA = 665, BB = 503 and CC = 113.

crack width that was observed in the sample from Prism A at RH of 15% was 1–5 μm (Fig. 7a). In the sample from Prism C, it was much more difficult to find secondary shrinkage microcracks, and they had widths generally less than 1 μm at 15% RH (Fig. 7b).

Because secondary shrinkage microcracks were formed in ESEM after cutting and grinding, the edges of these microcracks are sharp. As will be shown later, rims of microcracks that were present already before cutting and grinding (i.e. primary shrinkage microcracks) normally showed signs of abrasion due to cutting and grinding. Another characteristic of secondary shrinkage microcracks is the right angle (~90°) between the crack plane and the microscope sample surface (i.e. the cross-section surface).

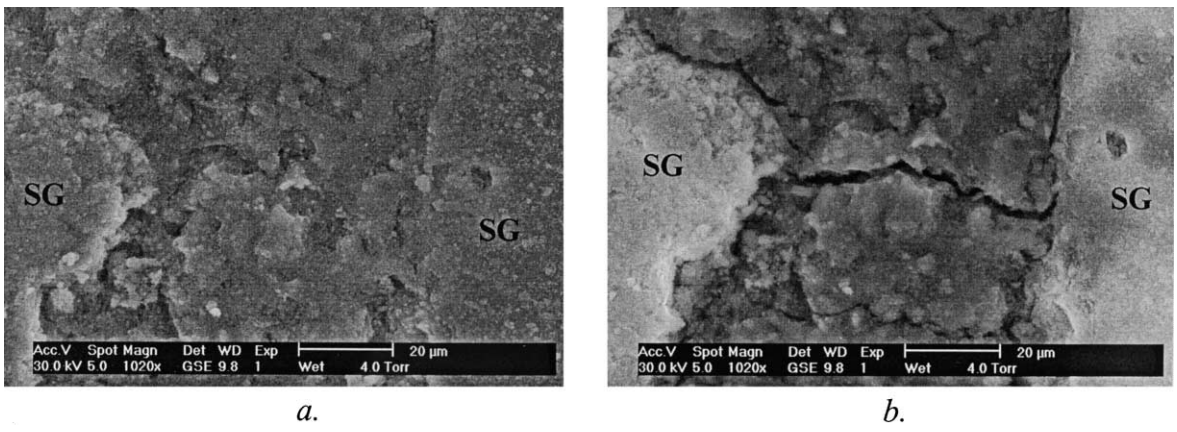

Fig. 6. ESEM micrographs of center of sample from wet-cured prism (A) taken at (a) RH of 70% (4.0 Torr, 3 °C) and (b) after 1/2 h drying in ESEM chamber at RH of 13% (4.0 Torr and 30 °C). The figure shows the development of secondary shrinkage microcracks. SG = sand grain.

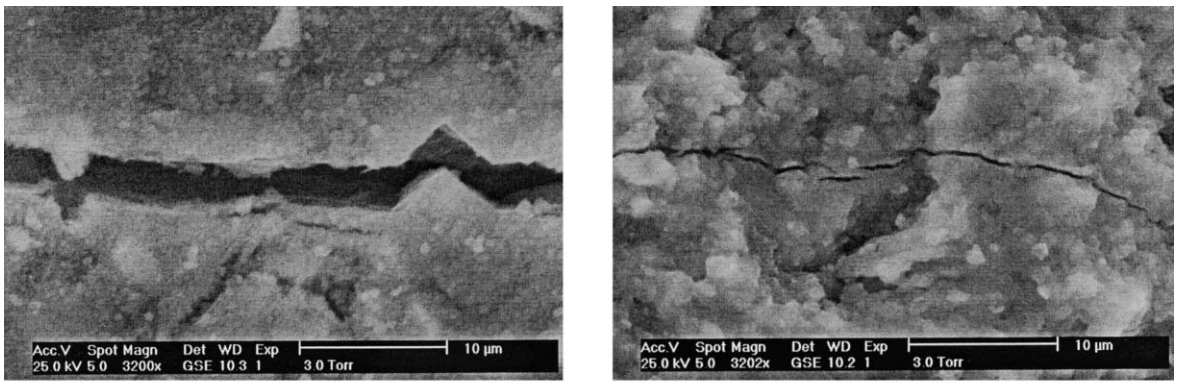

Fig. 7. ESEM micrographs of secondary shrinkage microcracks in centers of samples at RH of 15%. (a) Typical crack opening (1–5 μm) in sample of wet-cured prism (A) and (b) typical crack opening (< 1 μm) in sample of completely dried prism (C).

This is due to the fact that drying in ESEM causes self-restraining of the microscope sample. The self-restraining causes tensile stresses that are mainly directed parallel to the microscope sample surface. On the other hand, primary shrinkage microcracks can make any angle with respect the microscope sample surface, depending on the angle between the microcrack and cutting direction. The secondary shrinkage microcracks were not only due to self-restraining of the microscope sample but also due to the superimposed restraining effect of aggregates, as evidenced by the perpendicular orientation of these microcracks with respect to sand grains (Fig. 6b).

In the completely dried prism (C), primary shrinkage microcracks should be present near the prism surface as was shown with Method 1. The edges of ESEM sample of Prism C were carefully examined at high RH to see if primary shrinkage microcracks could be found. Some primary shrinkage microcracks were observed. They were visible not because of a crack opening, as can be expected because the microcracks were merely closed, but due to abrasion of the edges of the closed microcracks (see Fig. 8). After detailed inspection of the whole ESEM sample, it was found that the primary shrinkage microcracks were only seen close to the prism surface.

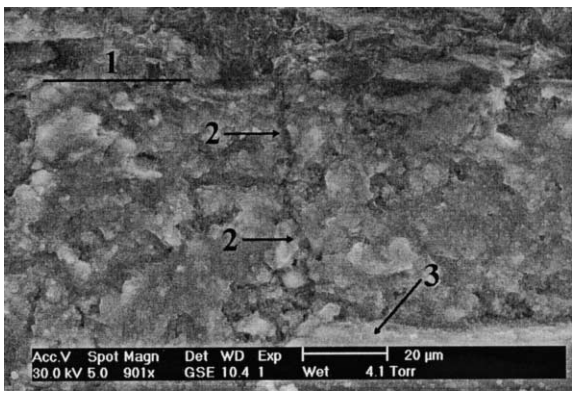

Fig. 8. ESEM micrograph of primary shrinkage microcrack on cross-section of the completely dried prism (C) at RH of 90% (4.1 Torr and 0 °C). 1 = embedded specimen surface, 2 = closed shrinkage microcrack abraded by grinding, 3 = sand grain.

4. Discussion

4.1. Comparison of results from different methods

From the results obtained with Method 2, it was seen that thin section AA showed the highest number of shrinkage microcracks, while thin section CC showed the least. BB showed a concentration of shrinkage microcracks in the center of the thin section and a rim of about 7 mm with much less shrinkage microcracks. This trend in shrinkage microcracking (shown by thin sections AA, BB and CC) indicates that the majority of these microcracks are probably secondary shrinkage microcracks. Primary shrinkage microcracking would probably have shown the reverse trend. Another indication that primary shrinkage microcracks only occurred near the edges of the thin section (i.e. near prism surface) is that the cutting damage was limited to this part (Section 3.2). In ESEM, it was observed that all microcracks present in the center of the ESEM samples were secondary shrinkage microcracks. The width of these microcracks in the sample from the wet-cured prism (A) was found to be significantly larger than the crack width in the sample of the completely dried prism (C).

If the results of Methods 2 and 3 are compared, it can be concluded that drying of the microscope sample surface lead to fewer and less wide secondary shrinkage microcracks in the sample from the dried Prism C (or in the dried part of the sample from Prism B) compared to the sample from the wet-cured Prism A. There is an easy explanation for this behavior. After making the cross-section in a wet-cured prism, drying of the sample surface will lead to a moisture gradient that causes differential shrinkage in the microscope sample and the formation of secondary shrinkage microcracks. In a dried prism, after making the cross-section,

additional drying of the sample surface is almost not possible, and therefore, no large differential shrinkage occurs. Consequently, compared to a wet sample, less secondary shrinkage microcracks with smaller width form on the microscope sample surface. This effect may disappear, however, when the sample is allowed to resaturate with water before secondary drying is applied.

From all observations, it can be concluded that the microcracks impregnated according to Method 1 probably comprised the complete primary shrinkage crack pattern in the prism. With ESEM, primary shrinkage microcracks were also only seen near the sample edge (i.e. near the prism surface). Furthermore, it was shown that dispersed shrinkage microcracks in the microscope samples prepared according to Method 2 and 3 were secondary shrinkage microcracks. Thus, in the studied mortar, all primary shrinkage microcracks apparently were connected to the prism surface and could be filled with epoxy from the prism surface.

4.2. The importance of the restraining effect of aggregate particles

The primary shrinkage microcracks shown with Method 1 are more or less perpendicular to the prism surface (see Figs. 4 and 8). This indicates that there was a large component of self-restraining of the prism in the cause of their formation [2]. As mentioned in Section 1, the restraining effect of the aggregates may also cause microcracking if tensile stresses are large enough. Apparently, the coarse fraction of the aggregates (4 mm) in the studied mortar was too small or the cement–aggregate ratio too low to cause shrinkage microcracking due to restraining effect of the aggregate particles alone. Moreover, the compressive stresses in the core of the prism due to self-restraining could also have had a hindering effect on microcrack formation by aggregate restraint.

An interesting question can now be posed. If cement-based materials would exist for which the restraining effect of aggregates alone is large enough to cause microcracking, would it then be possible to use Method 1 to impregnate the complete primary shrinkage microcrack pattern? To test whether this can be done, the following cement-based material was prepared. Cement paste with the same cement type and w/c ratio as the one used in the present mortar was mixed with spherical glass particles with a diameter of 6 mm. The aggregate–cement paste volume ratio was 0.5. The prism ($40 \times 40 \times 160$ mm) was dried at 20% RH and 30 °C from only one side (all other sides were sealed with adhesive tape) until 20% of the initial water content was lost. More information about these experiments can be found in Ref. [2]. As shown in Fig. 9, microcracks across the whole cross-section were impregnated. The random orientation of the radial paste microcracks indicates that they were mainly caused by the restraining effect of the glass spheres [2]. This example shows that even when aggregate restraining became important in causing microcracks, Method 1 could be used to impregnate the complete primary shrinkage microcrack pattern.

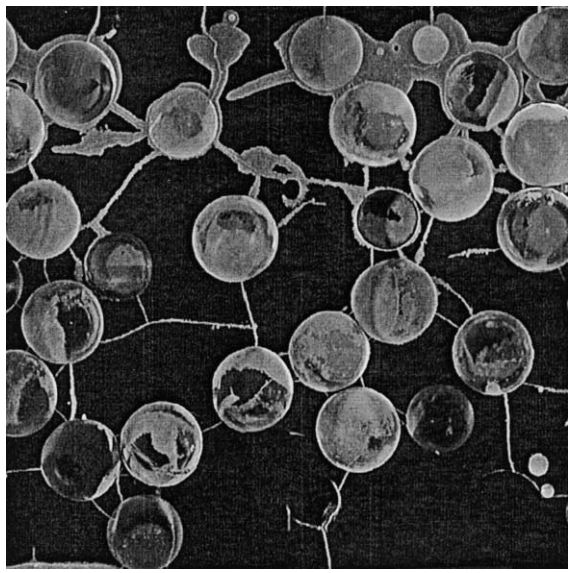

Fig. 9. FLM micrograph showing primary drying shrinkage microcracks on cross-section of dried cement-based material with glass spheres. Prism was impregnated according to Method 1. The paste directly adjacent to the microcracks is also impregnated with the epoxy, especially in the more dried upper part of the prism (bottom of image is casting surface). Frame size is 40×40 mm.

5. Conclusions

Experiments have been performed to find a method for observing primary drying shrinkage microcracks in a specimen using a ‘destructive’ microscopy technique. It was shown that in the studied mixtures with Method 1 (impregnation *before* making the cross-section), there was no risk of recording microcracks introduced by sample preparation. On the other hand, in fluorescent thin sections made according to Method 2 (impregnation *after* making the cross-section), secondary microcracks were introduced. The microcracks introduced by cutting in Method 2 obscured the primary drying shrinkage microcrack pattern, and in general, it is very difficult to distinguish between primary and secondary shrinkage microcracks in thin section prepared according Method 2.

With Method 3 (the ESEM method), it was possible to distinguish between primary and secondary shrinkage microcracks. However, the visibility of the primary shrinkage microcracks was in general very low, because swelling of the cement paste reduced the crack opening. Therefore, Method 1 appears to be the most reliable method to record primary drying shrinkage microcracking in cement-based materials. Even when microcracks occur in the bulk of the specimen solely due to the restraining effect of the aggregates, it seems possible to impregnate these microcracks according to Method 1.

Acknowledgments

The assistance of Mr. A.S. Elgersma in all experiments is gratefully acknowledged. Financial support was obtained from Delft Interfaculty Research Program "Micromechanics for macroscopic lifetime prediction" (DIOC-10).

References

[1] C.L. Hwang, J.F. Young, Drying shrinkage of Portland cement pastes: I. Microcracking during drying, Cem. Concr. Res. 14 (1984) 585–594.
[2] J. Bisschop, J.G.M. van Mier, Effect of aggregates on drying shrinkage microcracking in cement-based materials, UEF conference "Advances in Concrete and Cement", Mt. Tremblant, Canada, August, 2000 (Submitted to Concr. Sc. Eng.).
[3] P. Goltermann, Mechanical predictions of concrete deterioration—Part 2: Classification of crack patterns, ACI Mater. J. 92 (1) (1995) 58–63.
[4] K.O. Kjellsen, H.M. Jennings, Observations of microcracking in cement paste upon drying and rewetting by environmental scanning electron microscopy, Adv. Cem. Based Mater. 3 (1996) 14–19.
[5] H. Hornain, Microscopic observation of cracks in concrete—A new sample preparation technique using dye impregnation, Cem. Concr. Res. 26 (4) (1996) 573–583.
[6] H.C. Gran, Fluorescent liquid replacement technique. A means of crack detection and water:binder ratio determination in high strength concretes, Cem. Concr. Res. 25 (2) (1995) 1063–1074.
[7] E. Ringot, J.P. Ollivier, J.C. Maso, Characterisation of initial state of concrete with regard to microcracking, Cem. Concr. Res. 17 (1987) 411–419.
[8] J. Bisschop, J.G.M. van Mier, Quantification of shrinkage microcracking in young mortar with fluorescence light microscopy and ESEM, Proc. of the 7th Euroseminar on microscopy applied to building materials, June, DELFT University of Technology, Delft, The Netherlands, 1999, pp. 223–232.
[9] J. Bisschop, J.G.M. van Mier, Environmental scanning electron microscopy as tool to study shrinkage microcracks in cement-based materials, in Proc. of MRS 1999 Fall Meeting, Boston, vol. 589 (Materials Research Society, 2000).
[10] J.P. Ollivier, A non-destructive procedure to observe the microcracks of concrete by scanning electron microscopy, Cem. Concr. Res. 15 (1985) 1055–1060.
[11] P.J.R. Uwins, Environmental scanning electron microscopy, Mater. Forum 18 (1994) 51–75.
[12] G. Elssner, H. Hoven, G. Kiessler, P. Wellner, Ceramics and ceramic composites: materialographic preparation, Elsevier, New York, USA, 1999, pp. 2–6.